LUND UNIVERSITY

Inverse bounds and bulk properties of complex-valued two-component composites

Engström, Christian

2005

Link to publication

Total number of authors:
1

Inverse bounds and bulk properties of complex-valued two-component composites

Christian Engström

Department of Electroscience
Electromagnetic Theory
Lund Institute of Technology
Sweden
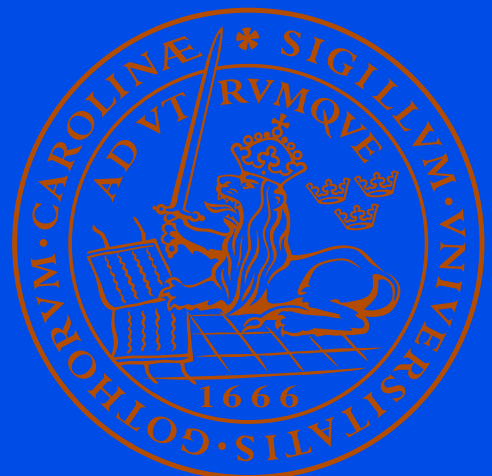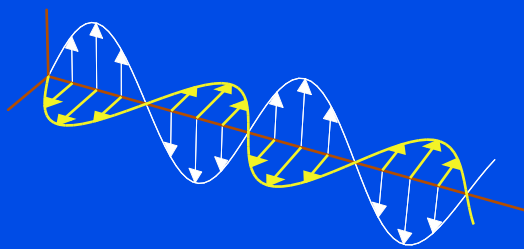
Christian Engström

Department of Electroscience
Electromagnetic Theory
Lund Institute of Technology
P.O. Box 118
SE-221 00 Lund
Sweden

Abstract

The bulk properties of composites are known to depend strongly on the microstructure. This dependence can be quantified in terms of a representation introduced by D. Bergman, which factorizes the geometry dependence from the contrast. Based on this analytic representation of the effective permittivity, we present a general scheme to estimate the micro structural parameters, such as the volume fraction and the anisotropy of two-component composites. The estimates are given as bounds, that is, the largest parameter region which is compatible with the available information. Thus, more information produces better estimates on the micro structural parameters. The method, that uses complex-valued measurements of bulk properties of the composite, is illustrated by numerical examples.

1 Introduction

In many cases of interest when considering the interaction of electromagnetic waves with composites the wavelength is much longer than the characteristic length of the microstructure. The composite then reacts to the slowly varying field in much the same way as a homogeneous material, with some effective material parameters.

The determination of the effective properties of composite materials, with known periodic geometry or from simulations of random materials, constitutes a classical problem in physics. In the case of a two component mixture, a representation formula that separate the dependence on the phases and the dependence on the microstructure was developed by Bergman [6], and Golden and Papanicolaou [20].

The structural information is associated with a spectral measure and much effort has been focussed on the reconstruction of this measure from a known geometry [17, 22, 27]. When the measure is calculated, a single integral gives the effective property for any value of the phases. One drawback is that a complete knowledge of the geometry rarely is available.

A direct approach to characterize the microstructure is in terms of an infinite set of correlation functions [4, 35]. Except for some special cases, the infinite set of correlation functions are not known and hence an exact solution is not possible. Using images of cross sections, some correlation functions can be estimated. When the material is finely scaled, the computation of the volume fraction is a large computational problem and calculations of higher order correlation functions is in general very demanding.

Instead of using correlation functions, information from measurements of one effective property can be used to improve bounds on a related property. Prager [33] used measurements of the effective magnetic permeability to improve the bounds on the thermal conductivity. These bounds are called cross-property bounds or coupled bounds. The pioneering work of Prager was followed by papers of Bergman [5, 6] and Milton [31], among others. The problem of bounding the structural parameters that characterize the microstructure from known values of an effective property is by some authors called inverse homogenization and the bounds are called inverse bounds.

Inverse bounds for the volume fraction were first derived in [29]. In recent years the representation formula introduced by Bergman [6] has been used to study the inverse problem. Explicit formulas for bounds on the volume fraction can in the case of measurements of lossy materials be found in reference [12]. If the measurements are on a real-valued effective property, the formulas for the volume fraction in reference [12] cannot be used. In the case of real valued measurements the author in reference [19] provide a schedule to derive inverse bounds and give explicit formulas for bounds on the three lowest moments of the measure, where the first moment corresponds to the volume fraction.

Various inverse algorithms for recovering the structural parameters (the spectral measure) of composites from experimental data have been developed [11, 13, 15]. In reference [16] the algorithm developed in [15] was successfully used to recovering the measure from 4000 reflectance data points.

The numerical algorithms are useful but one disadvantage with this approach is that we lose the concept of bounds. If we have limited information from measurements (few or inaccurate measurements), the numerical methods cannot recover the measure. Using the numerical approximations of the measure can then result in bounds on an effective property that are not valid.

In this paper inverse bounds using information from measurements of lossy materials are derived. These bounds are used to derive cross-property bounds, which are exemplified by a frequency dependent permittivity. We use and improve the geometry independent bounds on the structural parameters that were derived in [19]. In other words, restrictions on the moments of the measure are derived.

The asymptotic behaviour of the formulas in this paper are superior to the formulas in [19], but the formulas presented here cannot be used if the effective property is real-valued. The two papers complement each other and the formulas in the two papers can be combined.

2   Bounds on the effective permittivity

Assume that inside the composite the electric field $\boldsymbol{E}$ and the electric flux density $\boldsymbol{D}$ satisfy the constitutive relation

$$\boldsymbol{D}(\boldsymbol{x}) = \boldsymbol{\epsilon}(\boldsymbol{x})\boldsymbol{E}(\boldsymbol{x}). \qquad (2.1)$$

The permittivity matrix $\boldsymbol{\epsilon}$ is the description of the material on the fine scale, where $\boldsymbol{\epsilon}$ and thereby the fields oscillate rapidly. On a much larger scale the averaged fields have no oscillations on the length scale of the microstructure, since they are smoothed out, but they retain slow macroscopic variations.

We seek an effective permittivity matrix $\boldsymbol{\epsilon}^{\text{eff}}$ which relates the average of the electric displacement field $\langle \boldsymbol{D} \rangle$ to the average of the electric field $\langle \boldsymbol{E} \rangle$. The average is over a volume having size large compared with the microstructure.

In general the $\boldsymbol{D}$-field satisfies $\nabla \cdot \boldsymbol{D} = \rho$, where ρ is the charge density. Using for example a two-scale expansion [2, p. 138] of Maxwell's equations, we have $\nabla \times \boldsymbol{E} = 0$.

From the constitutive relation (2.1) follows that, for a charge-free region, the $\boldsymbol{E}$-field satisfy

$$\nabla \times \boldsymbol{E} = 0, \quad \nabla \cdot (\boldsymbol{\epsilon E}) = 0. \tag{2.2}$$

This system represents, besides dielectrics, several other physical phenomena, as electrical and thermal conductivity, magnetism, diffusion and flow in porous media.

Let $\langle \boldsymbol{\Psi} \rangle$ denote the average of the vector field $\boldsymbol{\Psi}$ over the unit cell $U = [0, 1[^d$ in d dimensions. If the $\boldsymbol{E}$-field is Lebesque integrable and the equations (2.2) are satisfied in a weak sense, the homogenization rule

$$\langle \boldsymbol{\epsilon E} \rangle = \boldsymbol{\epsilon}^{\text{eff}} \langle \boldsymbol{E} \rangle, \tag{2.3}$$

can be proven [23, p. 15].

The materials in this paper are assumed to be d-dimensional and to consist of two homogeneous, isotropic phases. The two-component material is locally modelled by the scalar relative permittivity

$$\epsilon(\epsilon_1, \epsilon_2) = \epsilon_1 \chi_1(\boldsymbol{x}) + \epsilon_2 \chi_2(\boldsymbol{x}), \tag{2.4}$$

where the components are isotropic with constant permittivity ϵ_1 and ϵ_2. We use complex valued permittivities and assume that the imaginary parts are greater or equal to zero.

The volume fraction of phase χ_i is denoted f_i and the characteristic function χ_i is defined as

$$\chi_i(\boldsymbol{x}) = \begin{cases} 1, & \boldsymbol{x} \text{ in phase } i \\ 0, & \text{otherwise} \end{cases}$$

and $f_1 + f_2 = 1$. When the composite is periodic and the characteristic function χ_1 is known, we can calculate $\boldsymbol{\epsilon}^{\text{eff}}$ from (2.2), (2.3) using a standard finite-element program, but in many cases the geometry is unknown. Another drawback with this approach is that the problem (2.2), (2.3) depends not only on the microstructure but also on the contrast. If we change the contrast all calculations need to be repeated.

2.1 Analytic representation of the effective matrix

Due to the homogeneity property $\boldsymbol{\epsilon}^{\text{eff}}(c\epsilon_1, c\epsilon_2) = c\boldsymbol{\epsilon}^{\text{eff}}(\epsilon_1, \epsilon_2)$, the effective permittivity depends on the ratio ϵ_1/ϵ_2. The main property of the solution to the problem in (2.2) and (2.3) is that the function

$$\frac{\boldsymbol{\epsilon}^{\text{eff}}(\epsilon_1, \epsilon_2)}{\epsilon_2} = \boldsymbol{\epsilon}^{\text{eff}}\left(\frac{\epsilon_1}{\epsilon_2}, 1\right) \tag{2.5}$$

is analytic in $\epsilon_1/\epsilon_2 \in \mathbb{C} \backslash] - \infty, 0]$ and that it maps the upper half-plane to the upper half-plane $i.e.$, the function $\boldsymbol{\epsilon}^{\text{eff}}/\epsilon_2$ is a Herglotz function [1]. The function $\boldsymbol{\epsilon}^{\text{eff}}/\epsilon_2$ has the Stieltjes-integral representation

$$\boldsymbol{\epsilon}^{\text{eff}}(\epsilon_1, \epsilon_2) = \epsilon_2 \mathbf{I} - \epsilon_2 \mathbf{G}(s), \tag{2.6}$$

where

$$\mathbf{G}(s) = \int_0^1 \frac{\mathrm{d}\mathbf{m}(y)}{s - y}, \quad s = \frac{\epsilon_2}{\epsilon_2 - \epsilon_1}. \tag{2.7}$$

The matrix valued measure $\mathbf{m}$ on $[0,1]$ is derived from the spectral measure of the operator $\Gamma = P\chi_1$, where $P = \nabla(-\Delta)^{-1}(\nabla\cdot)$. The operator Γ is bounded $\|\Gamma\| \leq 1$ and self-adjoint in $L^2(\mathrm{U})^d$ equipped with the scalar product $(\boldsymbol{\Psi}_1, \boldsymbol{\Psi}_2) = \langle \chi_1 \boldsymbol{\Psi}_1 \cdot \boldsymbol{\Psi}_2 \rangle$ [20]. The representation formula (2.6), valid for $s \notin [0,1]$, was introduced in the periodic case by Bergman [6] and generalized by Golden and Papanicolaou [20].

The measure $\mathbf{m}$ is a purely geometric quantity. It depends on the microstructure but not on the value of the two phases. If the microstructure is the same, the single integral (2.7) gives the effective permittivity, independent of the value of the phases. This is particularly useful when the permittivity is frequency or temperature dependent.

2.2   Bounds on ϵ^{eff} using Padé approximations

If the microstructure is only partly known, we can get bounds on the effective permittivities. When the permittivities of the two materials, together with the volume fraction f_1, are known, the effective permittivity is bounded by the harmonic and arithmetic means. If more structural information is known, we get tighter bounds as the Hashin-Shtrikman bounds and the Beran bounds.

We focus on the diagonal elements in the effective permittivity matrix and use the power series expansion

$$\boldsymbol{\epsilon}^{\mathrm{eff}} = \epsilon_2 \mathbf{F}(z), \qquad \mathbf{F}(z) = \sum_{n=0}^{\infty} \mathbf{c}_n z^n \tag{2.8}$$

where $z = -1/s = (\epsilon_1 - \epsilon_2)/\epsilon_2$ is the contrast. The series (2.8) is convergent in $|z| < 1$.

The integral (2.7) vanishes in the limit $s \to \infty$, implying $\mathbf{c}_0 = \mathbf{I}$. This is a consequence of (2.8), because $z = 0$ when $\epsilon_1 = \epsilon_2$, which means that we only have one material.

For $|s| > 1$ the function $(s - y)^{-1}$ has a power expansion in y/s. The integral $\mathbf{G}(s)$ then has the power expansion

$$\mathbf{G}(s) = \sum_{n=0}^{\infty} \frac{1}{s^{n+1}} \int_0^1 y^n \, \mathrm{d}\mathbf{m}(y). \tag{2.9}$$

The integral in this expression is, for $n = 0, 1, \ldots$, the (Hausdorff) moments of the measure $\mathbf{m}$. The coefficients $\mathbf{c}_n$ in the power series expansion (2.8) and the measure $\mathbf{m}$ are connected by the moments

$$\mathbf{c}_{n+1} = (-1)^n \int_0^1 y^n \, \mathrm{d}\mathbf{m}(y). \tag{2.10}$$

Since the measure $\mathbf{m}$ is defined on the compact set $[0,1]$ it follows that $\mathbf{m}$ is bounded and uniquely determined by the moments [1]. If all the moments are known, the

effective matrix is obtained from the series (2.8). Thus, the local information about $\epsilon_1 = \epsilon_2$ gives the effective permittivity independent of the contrast.

The volume fraction f_1 is given by the total weight [6, 20]

$$\mathbf{c}_1 = \int_0^1 \mathrm{d}\mathbf{m}(y) = f_1\mathbf{I}. \tag{2.11}$$

Higher-order moments depend on the geometrical structure. Bergman [6] derived the general constraint $\mathrm{Tr}\,\mathbf{c}_2 = -c_1(1 - c_1)$ and that, in the case of a statistically isotropic composite, the second moment is

$$\mathbf{c}_2 = -\int_0^1 y\,\mathrm{d}\mathbf{m}(y) = -\frac{c_1(1 - c_1)}{d}\mathbf{I}. \tag{2.12}$$

Higher-order moments can be calculated exactly in a few special cases; see for instance [14] or [17].

The power series (2.8) with coefficients given by the moments (2.10) defines a series of Stieltjes. Series of Stieltjes have known upper and lower bounds in the form of continued fractions or Padé approximations [1]. We use Padé approximations of the power series (2.8).

Let ϵ^{eff} be one of the diagonal elements in the matrix $\boldsymbol{\epsilon}^{\mathrm{eff}} = \epsilon_2\mathbf{F}(z)$. The $\epsilon_{p,q}$ Padé approximant to ϵ^{eff} is defined by the equation

$$\epsilon^{\mathrm{eff}}(z)Q(z) - P(z) = \mathcal{O}(z^{p+q+1}) \tag{2.13}$$

where P and Q are polynomials of degree at most p and q, respectively [1]. This equation gives us an approximation of the effective permittivity by the rational function

$$\epsilon_{p,q} = \frac{P(z)}{Q(z)} = \frac{a_0 + ... + a_p z^p}{1 + b_1 z + ...b_q z^q}. \tag{2.14}$$

When $\epsilon_2 > \epsilon_1$ and $N \geq 1$, the N-point upper bounds $\boldsymbol{\epsilon}_N^{\mathrm{U}}$ are obtained by forming the approximations

$$\boldsymbol{\epsilon}_{2M+1}^{\mathrm{U}} = \epsilon_2\boldsymbol{\epsilon}_{M+1,M}(\mathbf{F}), \quad \boldsymbol{\epsilon}_{2M}^{\mathrm{U}} = \epsilon_2\boldsymbol{\epsilon}_{M,M}(\mathbf{F}). \tag{2.15}$$

The inverse of the matrix $\boldsymbol{\epsilon}^{\mathrm{eff}}(\epsilon_1/\epsilon_2, 1)$ is analytic in $\epsilon_1/\epsilon_2 \in \mathbb{C}\backslash] - \infty, 0]$. The analyticity implies that it has a power series expansion in z. Lower bounds on $\boldsymbol{\epsilon}^{\mathrm{eff}}$ are given from Padé approximations of the series

$$\left(\frac{\boldsymbol{\epsilon}^{\mathrm{eff}}}{\epsilon_1}\right)^{-1} = \tilde{\mathbf{F}}(z), \quad \text{where} \quad \tilde{\mathbf{F}}(z) = \sum_{n=0}^{\infty} \tilde{\mathbf{c}}_n z^n. \tag{2.16}$$

The coefficients $\mathbf{c}_n$ and $\tilde{\mathbf{c}}_n$ in the two series are related according to

$$\tilde{\mathbf{c}}_0 = \mathbf{I}, \quad \tilde{\mathbf{c}}_1 = (1 - c_1)\mathbf{I}, \quad \tilde{\mathbf{c}}_n = -\sum_{k=0}^{n-1} \tilde{\mathbf{c}}_k \mathbf{c}_{n-k}. \tag{2.17}$$

The coefficient c_1 is the volume fraction of phase one (2.11) and $\tilde{c}_1$ is the volume fraction of phase two. The N-point lower bounds $\boldsymbol{\epsilon}_N^L$, when $\epsilon_2 > \epsilon_1$ and $N \geq 1$, are obtained from

$$\boldsymbol{\epsilon}_{2M+1}^L = \epsilon_1 [\boldsymbol{\epsilon}_{M+1,M}(\tilde{\mathbf{F}})]^{-1}, \quad \boldsymbol{\epsilon}_{2M}^L = \epsilon_1 [\boldsymbol{\epsilon}_{M,M}(\tilde{\mathbf{F}})]^{-1}. \tag{2.18}$$

For example the $\boldsymbol{\epsilon}_{1,0}$ Padé approximant of the expansion (2.16) is the harmonic mean

$$\boldsymbol{\epsilon}_1^L = \frac{\epsilon_1}{1 + \tilde{c}_1 z}\mathbf{I} = \left(\frac{f_1}{\epsilon_1} + \frac{f_2}{\epsilon_2}\right)^{-1}\mathbf{I} \tag{2.19}$$

and the $\boldsymbol{\epsilon}_{1,0}$ Padé approximant of (2.8) gives the arithmetic mean

$$\boldsymbol{\epsilon}_1^U = (\epsilon_2 + c_1\epsilon_2 z)\mathbf{I} = (f_1\epsilon_1 + f_2\epsilon_2)\mathbf{I}. \tag{2.20}$$

Wiener [39] first derived these bounds on an effective material parameter. In the same way the $\boldsymbol{\epsilon}_{1,1}$ Padé approximant of the expansion (2.16) is the lower bound

$$\boldsymbol{\epsilon}_2^L = \epsilon_1 [\tilde{c}_1\mathbf{I} - \tilde{\mathbf{c}}_2 z][\tilde{c}_1\mathbf{I} - \tilde{\mathbf{c}}_2 z + \tilde{c}_1^2 z\mathbf{I}]^{-1} \tag{2.21}$$

where $\tilde{\mathbf{c}}_2 = -\mathbf{c}_2 - c_1\tilde{c}_1\mathbf{I}$. The $\boldsymbol{\epsilon}_{1,1}$ Padé approximant of (2.8) gives the upper bound

$$\boldsymbol{\epsilon}_2^U = \epsilon_2 [c_1\mathbf{I} - \mathbf{c}_2 z + c_1^2 z\mathbf{I}][c_1\mathbf{I} - \mathbf{c}_2 z]^{-1}. \tag{2.22}$$

These bounds were first derived in [31]; see also [26, 37].

In the isotropic case, $\mathbf{c}_2 = -(c_1\tilde{c}_1/d)\mathbf{I}$, the two-point bounds (2.21) and (2.22) are equivalent to the Hashin-Shtrikman bounds [21] and the bounds $\boldsymbol{\epsilon}_3^L$, $\boldsymbol{\epsilon}_3^U$ reduce to the Beran bounds [3, 36]. The Padé approximations give a hierarchy of bounds that become progressively narrower as more structural information is used [1, 9, 32, 38]. The bounds (2.21) and (2.22) are optimal, since they are attained for a variety of geometries [7, 30]. In general, the bounds on the effective permittivity (2.15) and (2.18) can be improved by incorporating the phase exchange relation [24, 34]; see [31, 32].

2.3 Complex bounds on the permittivity

Let c_n be one of the diagonal elements in $\mathbf{c}_n$. In the general case when the values of the phases are complex, the real segment $l = \{c_n; c_n^{\min} \leq c_n \leq c_n^{\max}\}$ is for fixed values on $c_1, c_2, \ldots, c_{n-1}$ mapped by $\epsilon_n^L(c_n)$ and $\epsilon_n^U(c_n)$ on a circle or a line segment.

The minimum $c_n^{\min}$ and the maximum $c_n^{\max}$ are functions of the lower order parameters $c_1, c_2, \ldots, c_{n-1}$. The extreme values can be determined by varying the c_n parameter in the n-point bounds and using that the n-point bounds are forbidden to violate the $(n-1)$-point bounds. This procedure was used in reference [19].

For example, we get complex bounds from the lens-shaped region bounded by

$$\epsilon_2^L(\tilde{c}_2; \epsilon_1, \epsilon_2, \tilde{c}_1), \quad \epsilon_2^U(c_2; \epsilon_1, \epsilon_2, c_1) \tag{2.23}$$

with the structural parameter $\tilde{c}_2$ and c_2 varying between

$$c_2^{\min} = -c_1(1 - c_1), \quad c_2^{\max} = 0. \tag{2.24}$$

Alternatively, we can describe the bounds $\epsilon_n^{\mathrm{L}}(c_n)$ and $\epsilon_n^{\mathrm{U}}(c_n)$ in terms of the points through which the circle passes [8, 31]. Let $\mathrm{Arc}(z_0, z_1, z_2)$ denote the arc of a circle joining the points z_0 and z_1 that when extended passes through z_2. For example, the effective permittivity ϵ^{eff} is in the complex case bounded by the intersection of the circles

$$\mathrm{Arc}(\epsilon_1, \epsilon_1^{\mathrm{L}}, \epsilon_1^{\mathrm{U}}), \ \mathrm{Arc}(\epsilon_2, \epsilon_1^{\mathrm{L}}, \epsilon_1^{\mathrm{U}}). \tag{2.25}$$

We have $\epsilon_2^{\mathrm{L}} \to \epsilon_1$ and $\epsilon_2^{\mathrm{U}} \to \epsilon_2$ when $c_2 \to -\infty$. It follows that in terms of the structural parameters c_2, the circles are described by

$$\mathrm{Arc}(\epsilon_2^{\mathrm{L}}(-\infty), \epsilon_2^{\mathrm{L}}(c_2^{\mathrm{min}}), \epsilon_2^{\mathrm{L}}(c_2^{\mathrm{max}})), \ \mathrm{Arc}(\epsilon_2^{\mathrm{U}}(-\infty), \epsilon_2^{\mathrm{U}}(c_2^{\mathrm{min}}), \epsilon_2^{\mathrm{U}}(c_2^{\mathrm{max}})). \tag{2.26}$$

The arcs (2.25) or (2.26), defining the points through which the circles pass, provide a geometrical characterization of the bounds. The alternative representation of the arcs (2.23) gives, in terms of c_2, directly a parameterization of the lens-shaped boundary.

3 Inverse bounds and bulk properties

The task in inverse homogenization is in to calculate the structural parameters $\mathbf{c}_n$, or equally, the measure $\mathbf{m}$ given information from experiments.

When only measured values of the effective permittivity are known, the moments cannot be determined. Given a finite number of measurements, there exist in general several geometries that give the same $\boldsymbol{\epsilon}^{\mathrm{eff}}$. Moreover, any measurement contains noise, which limits the accuracy.

The measurements can be on one effective property of the material at different temperatures, or in a range of frequencies. It is also possible to get information from measurements of several related parameters, such as the permittivity, the permeability, and the thermal conductivity. The important thing is that the microstructure is the same.

Bounds on the volume fraction c_1, using information from measurements, were derived in [12, 19, 29]. In [12], the authors derived bounds on the volume fraction that are valid in the general anisotropic case and tighter bounds on the volume fraction when the material is statistically isotropic.

We focus on the diagonal elements in $\mathbf{c}_n$ and provide a method to derive bounds on any diagonal element c_n. Moreover, we give examples where c_1, c_2 and c_3 are bounded, using information from measurements. We assume that the measurements are on the effective permittivity ϵ^{eff} at different frequencies $\omega_0, \omega_1, \ldots, \omega_n$, although the measurements could very well pertain to several other physical parameters associated with the same micro-structure [32].

The bounds on the structural parameters c_n give geometrical information of the composite, but in many cases the composites effective bulk properties as a function of frequency or temperature is what is desired. The bounds on the structural parameters imply cross-property bounds on the effective properties, which gives bounds on the effective permittivity at all frequencies where the homogenization theory is valid.
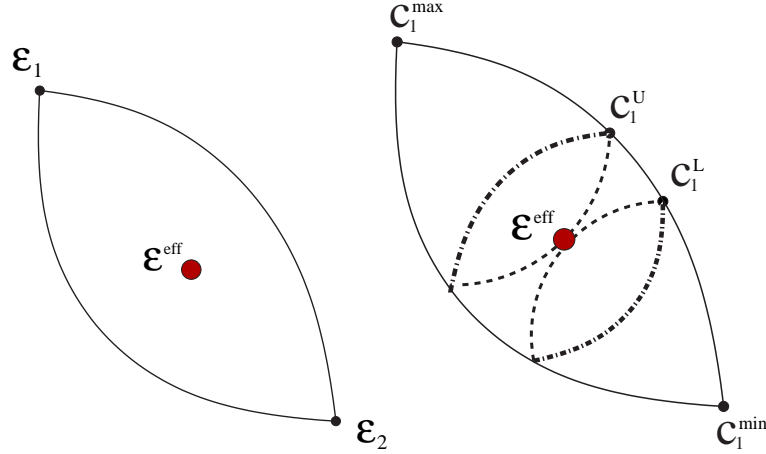
Figure 1: Left: The effective permittivity ϵ^{eff} is bounded by $\epsilon_1^{\mathrm{L}}(c_1)$ and $\epsilon_1^{\mathrm{U}}(c_1)$. Right: For some value $c_1 = c_1^{\mathrm{L}}$, the effective permittivity ϵ^{eff} is on the boundary of $\epsilon_2^{\mathrm{L}}(c_2; c_1^{\mathrm{L}}, \omega_0)$, $\epsilon_2^{\mathrm{U}}(c_2; c_1^{\mathrm{L}}, \omega_0)$ and for some value $c_1 = c_1^{\mathrm{U}}$, the effective permittivity is on the boundary of $\epsilon_2^{\mathrm{L}}(c_2; c_1^{\mathrm{U}}, \omega_0)$, $\epsilon_2^{\mathrm{U}}(c_2; c_1^{\mathrm{U}}, \omega_0)$.

3.1 Geometry independent inverse bounds

The volume fraction $f_1 = c_1$ is bounded between zero and one. The higher-order parameters depend on the geometry, and bounds on c_n are not known a priori. In the general anisotropic case, the parameter c_2 is bounded by

$$-c_1 \tilde{c}_1 \le c_2 \le 0, \tag{3.1}$$

where $\tilde{c}_1 = 1 - c_1$. This geometry independent bound on c_2 was proven in reference [10]. The author uses properties of the scalar measure $m(y)$ to derive the moment constraint

$$0 \le \int_0^1 y \, \mathrm{d}m(y) \le f_1 f_2, \tag{3.2}$$

which is equivalent to (3.1), see also [6, 19, 25, 35].

In [19] the author provides a general scheme to derive bounds on the structural parameter c_n, using lower-order parameters, see Section 2.3 for the connection to complex bounds. The bounds on the c_n-parameters depend on the lower-order parameters $c_1, \ldots, c_{n-1}$.

Here, we use that c_3 is bounded by $c_3^{\min} \le c_3 \le c_3^{\max}$ with [19]

$$c_3^{\min} = \frac{c_2^2}{c_1}, \quad c_3^{\max} = -c_2 \left(1 + \frac{c_2}{\tilde{c}_1} \right) \tag{3.3}$$

and that the structural parameter c_4 is bounded by $c_4^{\min} \le c_4 \le c_4^{\max}$ where [19]

$$c_4^{\min} = \frac{c_2^3 + \tilde{c}_1 c_2^2 + c_2 c_3(\tilde{c}_1 - c_1) + c_3(c_3 - c_1 \tilde{c}_1)}{c_2 + c_1 \tilde{c}_1}, \quad c_4^{\max} \le \frac{c_3^2}{c_2}. \tag{3.4}$$

3.2 Bounds using one measurement

Assume that the complex value of one effective parameter $\epsilon^{\text{eff}}(\omega_0)$ is measured for some frequency ω_0. We derive bounds on c_1 together with bounds on the effective parameter $\epsilon^{\text{eff}}(\omega_1)$, when $\epsilon_1(\omega_0)$, $\epsilon_2(\omega_0)$, $\epsilon_1(\omega_1)$ and $\epsilon_2(\omega_1)$ are known constants. If the volume fraction c_1 is known, the parameter c_2 is bounded and so on.

We assume that at least one of the phases has a positive imaginary part. That is, we assume that there are losses somewhere in the composite material. In the case of real values of both the phases, the method developed in reference [19] can be used to obtain bounds on c_1 and on ϵ^{eff}. In the lossless case, a direct calculation of the inverse of $\epsilon_1^{\text{L}}(c_1)$ and $\epsilon_1^{\text{U}}(c_1)$ is possible. When the measurements are complex-valued, a different approach is needed.

The measured value $\epsilon^{\text{eff}}(\omega_0)$ is inside the lens-shaped region bounded by

$$\epsilon_1^{\text{L}}(c_1; \omega_0) = \frac{1}{1 + \tilde{c}_1 z(\omega_0)}, \quad \epsilon_1^{\text{U}}(c_1; \omega_0) = \epsilon_1(\omega_0) + c_1 \epsilon_2(\omega_0) z(\omega_0), \quad (3.5)$$

with $z(\omega_0) = (\epsilon_1(\omega_0) - \epsilon_2(\omega_0))/\epsilon_2(\omega_0)$, $\tilde{c}_1 = 1 - c_1$, and $0 \leq \tilde{c}_1 \leq 1$. The boundary of the region is depicted in Figure 1.

For some values of c_1 and c_2, the effective parameter $\epsilon^{\text{eff}}(\omega_0)$ is on the curve $\epsilon_2^{\text{U}}(c_2, c_1; \omega_0)$, see Figure 1. The parameters c_1 and c_2 then solve the equation

$$\epsilon^{\text{eff}}(\omega_0) = \epsilon_2(\omega_0) \frac{c_1 - c_2 z(\omega_0) + c_1^2 z(\omega_0)}{c_1 - c_2 z(\omega_0)}, \quad (3.6)$$

with $0 \leq c_1 \leq 1$ and $-c_1 \tilde{c}_1 \leq c_2 \leq 0$.

At the minimum volume fraction $c_1 = 0$ and at the maximum volume fraction $c_1 = 1$, the ϵ_2^{U}-bound reduces to

$$\epsilon_2^{\text{U}}(0, c_2) = \epsilon_2^{\text{U}}(0, 0) = \epsilon_1^{\text{U}}(0) = \epsilon_2, \quad \epsilon_2^{\text{U}}(1, c_2) = \epsilon_2^{\text{U}}(1, 0) = \epsilon_1^{\text{U}}(1) = \epsilon_1, \quad (3.7)$$

which implies that the equation (3.6) has the solutions

$$\epsilon_2 = \epsilon_2^{\text{U}}(0, 0) = \epsilon^{\text{eff}}, \quad \epsilon_1 = \epsilon_2^{\text{U}}(1, 0) = \epsilon^{\text{eff}}. \quad (3.8)$$

By multiplying (3.6) with the denominator in ϵ_2^{U} we obtain

$$(c_1 - c_2 z)\epsilon^{\text{eff}} = \epsilon_2(c_1 - c_2 z + c_1^2 z^2). \quad (3.9)$$

We assume that $\epsilon^{\text{eff}} \neq \epsilon_1$ and look for solutions to the equation (3.9) when $0 \leq c_1 \leq 1$ and $-c_1 \tilde{c}_1 \leq c_2 \leq 0$. Taking the real and imaginary part of (3.9), which is quadratic in c_1 and linear in c_2, gives one solution (c_1, c_2) except for the trivial solution $(c_1, c_2) = (0, 0)$.

The calculated value on c_1 is a lower bound $c_1^{\text{L}}(\omega_0)$ on the volume fraction c_1. Explicitly, the volume fraction is bounded from below by

$$c_1^{\text{L}} = \text{Im}(z) \frac{(\text{Im}(\epsilon^{\text{eff}}) - \text{Im}(\epsilon_2))^2 + (\text{Re}(\epsilon^{\text{eff}}) - \text{Re}(\epsilon_2))^2}{|z|^2 (\text{Im}(\epsilon^{\text{eff}}) \text{Re}(\epsilon_2) - \text{Re}(\epsilon^{\text{eff}}) \text{Im}(\epsilon_2))}. \quad (3.10)$$

In the same way, for some values of $\tilde{c}_1$ and $\tilde{c}_2$, the effective parameter $\epsilon^{\text{eff}}(\omega_0)$ is on the curve $\epsilon_2^{\text{L}}(\tilde{c}_2, \tilde{c}_1; \omega_0)$. That is, we solve the equation

$$\epsilon^{\text{eff}}(\omega_0) = \epsilon_1(\omega_0) \frac{\tilde{c}_1 - \tilde{c}_2 z(\omega_0)}{\tilde{c}_1 - \tilde{c}_2 z(\omega_0) + \tilde{c}_1^2 z(\omega_0)}, \tag{3.11}$$

when $0 \leq \tilde{c}_1 \leq 1$ and $-\tilde{c}_1(1 - \tilde{c}_1) \leq \tilde{c}_2 \leq 0$.

At the end-points $(c_1, c_2) = (0, 0)$ and $(c_1, c_2) = (1, 0)$ the equation (3.11) has the solutions

$$\epsilon_1 = \epsilon_2^{\text{L}}(0, 0) = \epsilon^{\text{eff}}, \quad \epsilon_2 = \epsilon_2^{\text{L}}(1, 0) = \epsilon^{\text{eff}}. \tag{3.12}$$

Assume that $\epsilon^{\text{eff}} \neq \epsilon_2$ and multiply (3.11) with the denominator in ϵ_2^{L}. The resulting equation has one solution except for the trivial solution $(\tilde{c}_1, \tilde{c}_2) = (0, 0)$.

The solution to the equation $\epsilon^{\text{eff}}(\omega_0) = \epsilon_2^{\text{L}}(\tilde{c}_1, \tilde{c}_2)$ and the relation $c_1 = 1 - \tilde{c}_1$ gives an upper bound $c_1^{\text{U}}(\omega_0)$ on the volume fraction c_1. Explicitly, the volume fraction is bounded from above by

$$c_1^{\text{U}} = 1 - \text{Im}(z) \frac{(\text{Im}(\epsilon^{\text{eff}}) - \text{Im}(\epsilon_1))^2 + (\text{Re}(\epsilon^{\text{eff}}) - \text{Re}(\epsilon_1))^2}{|z|^2 (\text{Re}(\epsilon^{\text{eff}}) \text{Im}(\epsilon_1) - \text{Im}(\epsilon^{\text{eff}}) \text{Re}(\epsilon_1))}. \tag{3.13}$$

The derived bounds (3.10) and (3.13), on the volume fraction are equivalent to the bounds in reference [12]. Here we use a different method, which seems to be easier to generalize.

If $c_1 = c_1^{\text{L}}$, the measured value $\epsilon^{\text{eff}}(\omega_0)$ is equal to ϵ_2^{U} for some value of c_2. If $c_1 = c_1^{\text{U}}$ the effective permittivity $\epsilon^{\text{eff}}(\omega_0)$ is equal to ϵ_2^{L} for some value on c_2. The effective permittivity is bounded by the one-point bounds $\epsilon_1^{\text{L}}(c_1)$ and $\epsilon_1^{\text{U}}(c_1)$. From the calculations above and Figure 1, it follows that the effective permittivity also is bounded by the two-point bounds

$$\epsilon_2^{\text{L}}(c_2, c_1^{\text{L}}), \quad \text{with} \quad -c_1^{\text{L}}(1 - c_1^{\text{L}}) \leq c_2 \leq 0 \tag{3.14}$$

and

$$\epsilon_2^{\text{U}}(c_2, c_1^{\text{U}}), \quad \text{with} \quad -c_1^{\text{U}}(1 - c_1^{\text{U}}) \leq c_2 \leq 0. \tag{3.15}$$

These, bounds can for example be used to check the volume fraction in experiments when it is difficult to determine the volume fraction from direct measurements. If we measure the lossy permittivity for more than one frequency, the minimum of the calculated bounds on c_1 is the optimal.

3.2.1 Asymptotic behaviour

Write c_2 on the form $c_2 = -\alpha c_1 \tilde{c}_1$, $0 \leq \alpha \leq 1$ and let $\epsilon_1 = 1$ and $\epsilon_2 = 1 + \delta w$, where w is a complex number with non-zero imaginary part and modulus one. Using the expansion (2.8), the asymptotic behaviour when $\delta \to 0$ is

$$c_1^{\text{U}} - c_1^{\text{L}} = c_1 \hat{c}_1 \alpha(1 - \alpha)\delta^2 + \mathcal{O}(\delta^3). \tag{3.16}$$

For a fixed δ, the difference is smal when the c_2 parameter is close to the end points (3.1), and when the volume fraction $c_1 = f_1$ is close to its end points.
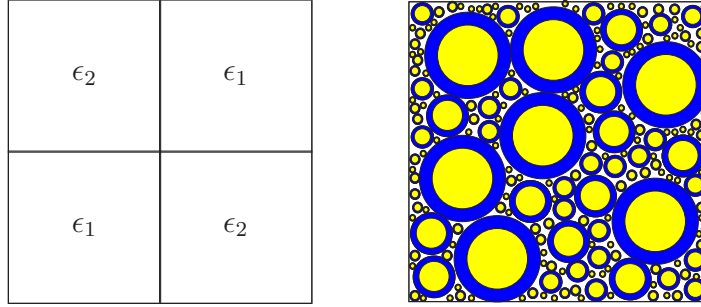
Figure 2: Left: The checkerboard structure, a two-dimensional and periodic problem. Right: The Hashin structure. Coated spheres, that are composed of a spherical core of permittivity ϵ_2 surrounded by a concentric shell of permittivity ϵ_1.

In the case of real valued phases, the parameter c_1 is bounded by [19]

$$c_1^{\mathrm{L}} = \frac{1/\epsilon^{\mathrm{eff}} - 1/\epsilon_2}{1/\epsilon_1 - 1/\epsilon_2}, \quad c_1^{\mathrm{U}} = \frac{\epsilon_2 - \epsilon^{\mathrm{eff}}}{\epsilon_2 - \epsilon_1}. \tag{3.17}$$

To procead, let $\epsilon_1 = 1$ and $\epsilon_2 = 1 + \delta$. Using the expansion (2.8), the asymptotic behavior when $\delta \to 0$ is in the lossless case given by

$$c_1^{\mathrm{U}} - c_1^{\mathrm{L}} = c_1 \hat{c}_1 \delta + \mathcal{O}(\delta^2). \tag{3.18}$$

The convergence is faster in the complex-valued case, which in many cases of interest implies much tighter bounds on the volume fraction. One interpretation of the result is that a measurement of a complex value contains more information compared to a measurement of a real value.

3.2.2 Examples

As a first illustration of the theory presented above, assume that one of the phases is a frequency independent material $\epsilon_1(\omega) = 3$, in the chosen range of frequencies. Moreover, phase two is lossy and measured at the frequencies ω_0, ω_1 and ω_2. We use the checkerboard structure and the Hashin structure, see Figure 2, to exemplify the method.

Phase two has the value $\epsilon_2(\omega_0) = 4.1 + 4.5\mathrm{i}$ at frequency ω_0. The checkerboard structure has the exact effective permittivity [32]

$$\epsilon_{\mathrm{C}}^{\mathrm{eff}}(\omega) = \sqrt{\epsilon_1(\omega)\epsilon_2(\omega)}. \tag{3.19}$$

It is interesting to notice that the checkerboard structure corresponds exactly to Bruggemans formula [32] at the percolation threshold $c_1 = 0.5$.

As described above, the solutions of the equations $\epsilon_{\mathrm{C}}^{\mathrm{eff}} = \epsilon_2^{\mathrm{L}}$ and $\epsilon_{\mathrm{C}}^{\mathrm{eff}} = \epsilon_2^{\mathrm{U}}$ bounds the volume fraction c_1. Figure 3 shows the bounds on $\epsilon_{\mathrm{C}}^{\mathrm{eff}}(\omega_1)$, when $\epsilon_2(\omega_1) =$
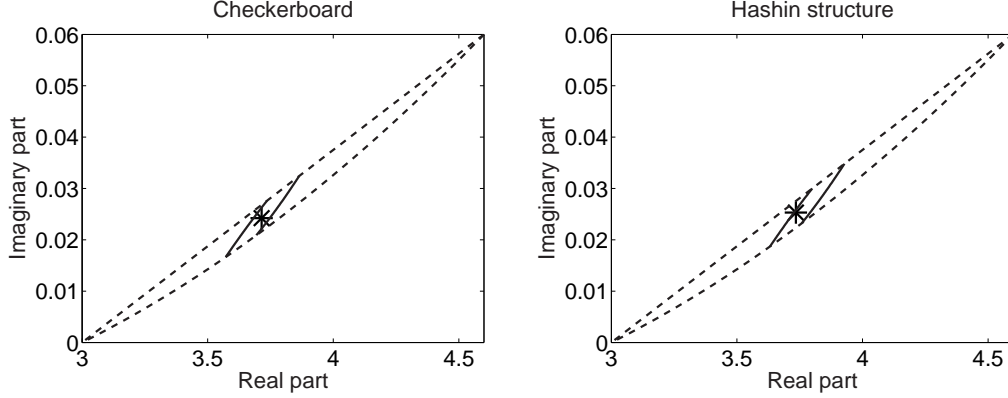
Figure 3: The star to the left is the effective permittivity in the checkerboard case and the star to the right corresponds to ϵ^{eff} for the Hashin structure. In both figures, the dashed lines $\epsilon_1^{\text{L}}(c_1)$ and $\epsilon_1^{\text{U}}(c_1)$ bounds $\epsilon^{\text{eff}}(\omega_1)$ and the solid lines are the tighter bound $\epsilon_2^{\text{L}}(c_2; c_1^{\text{L}})$ and $\epsilon_2^{\text{U}}(c_2; c_1^{\text{U}})$.

$4.6 + 0.06\text{i}$ is known and the bounds on c_1 are calculated to $c_1^{\text{L}}(\omega_0) = 0.46$ and $c_1^{\text{U}}(\omega_0) = 0.54$. The exact value on the volume fraction is $c_1 = 0.5$.

The Hashin structure [32], see Figure 2, in d-dimensions has the effective permittivty

$$\epsilon_{\text{H}}^{\text{eff}}(\omega) = \epsilon_1(\omega) \frac{(d-1)c_1(\epsilon_1(\omega) - \epsilon_2(\omega)) + d\epsilon_2(\omega)}{d\epsilon_1(\omega) + c_1(\epsilon_2(\omega) - \epsilon_1(\omega))}. \tag{3.20}$$

We consider the three-dimensional case, $d = 3$, with the volume fraction $c_1 = 0.5$. Using the value of ϵ_1, ϵ_2 and $\epsilon_{\text{H}}^{\text{eff}}$ at $\omega = \omega_0$ the bounds on c_1 are calculated to $c_1^{\text{L}}(\omega_0) = 0.42$ and $c_1^{\text{U}}(\omega_0) = 0.50$. Figure 3 shows the bounds on $\epsilon_{\text{H}}^{\text{eff}}(\omega_1)$ when $\epsilon_2(\omega_1)$ is known.

3.2.3   Bounds when the volume fraction is known

If the volume fraction c_1 is known, we obtain in the same way, bounds on c_2. The measured value $\epsilon^{\text{eff}}(\omega_0)$ is bounded by the lens-shaped region $\epsilon_2^{\text{L}}(c_2; \omega_0)$ and $\epsilon_2^{\text{U}}(c_2; \omega_0)$, with $-c_1 \tilde{c}_1 \leq c_2 \leq 0$.

For some values of c_2 and c_3, the effective parameter $\epsilon^{\text{eff}}(\omega_0)$ is on the boundary of $\epsilon_3^{\text{U}}(c_2, c_3; \omega_0)$, which is given by the Padé approximation $\epsilon_{1,1}$ of the series (2.8). On the curve, the parameters c_2 and c_3 satisfy the equation

$$\epsilon^{\text{eff}}(\omega_0) = \epsilon_2 \frac{c_2 + c_1 c_2 z + c_2^2 z^2 - c_3 z(1 + c_1 z)}{c_2 - c_3 z}, \tag{3.21}$$

with $-c_1 \tilde{c}_1 \leq c_2 \leq 0$ and $c_2^2/c_1 \leq c_3 \leq -c_2(1 + c_2/\tilde{c}_1)$.

At the minimum, $c_2 = -c_1 \tilde{c}_1$, the equation (3.21) has the solution

$$\epsilon_1^{\text{L}}(c_1) = \epsilon_2^{\text{U}}(c_2^{\text{min}}) = \epsilon_3^{\text{U}}(c_2^{\text{min}}, c_1(1 - c_1)^2) = \epsilon^{\text{eff}} \tag{3.22}$$

and at the maximum $c_2 = 0$ the solution to the equation is

$$\epsilon_1^U(c_1) = \epsilon_2^U(c_2^{\max}) = \epsilon_3^U(c_2^{\max}, 0) = \epsilon^{\text{eff}}. \tag{3.23}$$

By multipling (3.21) with the denominator in ϵ_3^U an equation quadratic in c_2 and linear in c_3 is obtained. Assume that $\epsilon^{\text{eff}} \neq \epsilon_1^L(c_1)$. Taking the real and imaginary part gives one solution (c_2, c_3) except for the trivial solution when $(c_2, c_3) = (0, 0)$ The calculated value on c_2 is an upper bound $c_2^U(\omega_0)$ on the structural parameter c_2.

Analogously, for some values of $\tilde{c}_2$ and $\tilde{c}_3$, the effective parameter $\epsilon^{\text{eff}}(\omega_0)$ is located on the boundary of $\epsilon_3^L(\tilde{c}_2, \tilde{c}_3; \omega_0)$, which is given by the Padé approximation $\epsilon_{1,1}$ of the series (2.16). That is, the equation

$$\epsilon^{\text{eff}}(\omega_0) = \epsilon_1 \frac{\tilde{c}_2 - \tilde{c}_3 z}{\tilde{c}_2 + \tilde{c}_1 \tilde{c}_2 z + \tilde{c}_2^2 z^2 - \tilde{c}_3 z(1 + \tilde{c}_1 z)}, \tag{3.24}$$

is solved with respect to $\tilde{c}_2$ and $\tilde{c}_3$. Using that the coefficients c_n and $\tilde{c}_n$ are related by (2.17), and solving the equation $\epsilon^{\text{eff}}(\omega_0) = \epsilon_3^L(c_2, c_3)$ gives a lower bound $c_2^L(\omega_0)$ on the structural parameter c_2. As before, the equation has one solution, except for the cases when $\epsilon^{\text{eff}} = \epsilon_1^L(c_1)$ and when $\epsilon^{\text{eff}} = \epsilon_1^U(c_1)$.

It is possible to derive explicit formulas for c_2^L and c_2^U but they contain many terms and will for this reason not be presented.

The effective permittivity is bounded by the two-point bounds $\epsilon_2^L(c_2)$ and $\epsilon_1^U(c_2)$. We have shown that the effective permittivity also is bounded by the three-point bounds

$$\epsilon_3^L(c_3, c_2^U), \quad \text{with} \quad \frac{c_2^U}{c_1} \le c_3 \le -c_2^U \left(1 + \frac{c_2^U}{1 - c_1}\right) \tag{3.25}$$

and

$$\epsilon_3^U(c_3, c_2^L), \quad \text{with} \quad \frac{c_2^L}{c_1} \le c_3 \le -c_2^L \left(1 + \frac{c_2^L}{1 - c_1}\right), \tag{3.26}$$

where c_2^U is calculated from (3.21) and c_2^L is the solution to equation (3.24). The bounds on c_3 are given by (3.3).

In many cases of interest, the composite is known to be isotropic, $c_2 = -c_1 \hat{c}_1/d$. The bounds on c_2 can then be used to check experimental data. If the volume fraction c_1 is known and $-c_1 \hat{c}_1/d$ does not belong to the interval $[c_2^L, c_2^U]$, the experimental value on ϵ^{eff} is incousistent with the bounds.

3.2.4 Examples

The checkerboard structure and the Hashin structure, with the same values on the phases as before, are used to illustrate the method.

The checkerboard has volume fraction $c_1 = 0.5$, which is assumed to be known. Figure 4 shows bounds on $\epsilon^{\text{eff}}(\omega_1)$, when the bounds on c_2 are calculated to $c_2^L(\omega_0) = -0.135$ and $c_2^U(\omega_0) = -0.115$. The checkerboard problem is two-dimensional and isotropic. The second moment, (2.12), with $c_1 = 0.5$ is then exactly $c_2 = -1/8 = -0.125$.
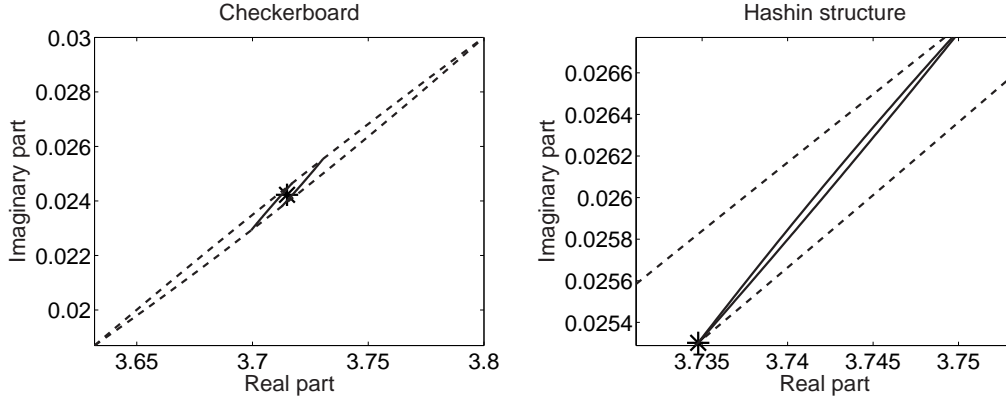
Figure 4: The star to the left is the effective permittivity in the checkerboard case and the star to the right corresponds to ϵ^{eff} for the Hashin structure. In both figures, the dashed lines $\epsilon_2^{\mathrm{L}}(c_2)$ and $\epsilon_2^{\mathrm{U}}(c_2)$ bounds $\epsilon^{\mathrm{eff}}(\omega_1)$ and the solid lines are the tighter bounds $\epsilon_3^{\mathrm{L}}(c_3; c_2^{\mathrm{U}})$ and $\epsilon_2^{\mathrm{U}}(c_3; c_2^{\mathrm{L}})$.

The Hashin structure is three-dimensional and isotropic. Using $c_1 = 0.5$, the second moment is $c_2 = -1/12 \approx -0.0833$. In this case the solution of the equations (3.21) and (3.24), when $c_1 = 0.5$ is known, determines c_2 numerically. The lower bound and the upper bound on c_2 have fifteen digits in common, when the equations are solved with Mathematica (`www.wolfram.com`). In the following section, we use the approximative value $c_2 = c_2^{\mathrm{U}}(\omega_0) = c_2^{\mathrm{L}}(\omega_0) = -0.0833$. Figure 4 shows bounds on $\epsilon^{\mathrm{eff}}(\omega_1)$ when $\epsilon_2(\omega_1) = 4.6 + 0.06\mathrm{i}$ is known.

3.2.5 Bounds on isotropic materials

If the volume fraction c_1 together with the c_2 parameter are known, (for example if the material is isotropic, $\mathbf{c_2} = -(c_1\tilde{c}_1/d)\mathbf{I}$), the equations

$$\epsilon^{\mathrm{eff}}(\omega_0) = \epsilon_4^{\mathrm{U}}(c_3, c_4; \omega_0), \quad \epsilon^{\mathrm{eff}}(\omega_0) = \epsilon_4^{\mathrm{L}}(\tilde{c}_3, \tilde{c}_4; \omega_0) \tag{3.27}$$
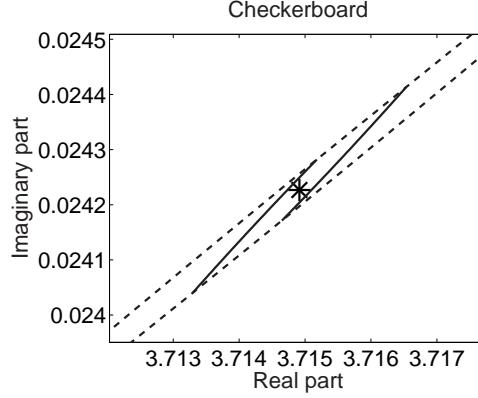
give us bounds on c_3. In general, if the structural parameters $c_1, c_2, \ldots, c_n$ are known, we obtain bounds on c_{n+1} from the equations

$$\epsilon^{\mathrm{eff}}(\omega_0) = \epsilon_{n+1}^{\mathrm{U}}(c_{n+1}, c_{n+2}; \omega_0), \quad \epsilon^{\mathrm{eff}}(\omega_0) = \epsilon_{n+1}^{\mathrm{L}}(\tilde{c}_{n+1}, \tilde{c}_{n+2}; \omega_0). \tag{3.28}$$

We can also get bounds on one structural parameter c_n if $c_1, c_2, \ldots, c_{n-1}$ and c_{n+1} are known. For example, if the material is known to be isotropic $c_2 = -c_1(1-c_1)/d$, the Hashin-Shtrikman bounds give us tighter bounds on the volume fraction than the solution to (3.6).

3.2.6 Examples

The bounds on $c_1(\omega_0)$, for the checkerboard structure above were calculated to $c_1^{\mathrm{L}}(\omega_0) = 0.46$ and $c_1^{\mathrm{U}}(\omega_0) = 0.54$. We now use that $c_2 = -0.125$ and solve $\epsilon^{\mathrm{eff}}(\omega_0) =$

Figure 6: Left: The union of the regions $\epsilon_2^L(c_2; c_1^L)$, $\epsilon_2^U(c_2; c_1^L)$ and $\epsilon_2^L(c_2; c_1^U)$, $\epsilon_2^U(c_2; c_1^U)$ bounds $\epsilon^{\text{eff}}(\omega_1)$. Right: For some values on $c_2 = c_2(c_1)$, the effective permittivity $\epsilon^{\text{eff}}(\omega_1)$ is on the boundary of $\epsilon_3^L(c_3; c_2(c_1), c_1, \omega_1)$, $\epsilon_3^U(c_3; c_2(c_1), c_1, \omega_1)$. The two lens-shaped regions correspond to two different values on the volume fraction c_1.

solution determines c_3 numerically. The lower bound c_3^L and the maximum c_3^{max} have sixteen digits in common, when the equations are solved with Mathematica (www.wolfram.com).

The properties $\epsilon_3^U(c_3^{\text{max}}) = \epsilon_2^L(c_2, c_1)$ and $\epsilon_3^L(c_3^{\text{max}}) = \epsilon_2^L(c_2, c_1)$ implies $\epsilon^{\text{eff}} = \epsilon_2^L(c_2, c_1)$.

When the composite is isotropic, the lower bound ϵ_2^L is equivalent with the Maxwell-Garnett formula [28, 32]. This formula, commonly used by experimentalists is a good approximation formula if c_3 is close to c_3^{max}.

3.3 Bounds using two measurements

We cannot determine bounds on more than one structural parameter with information from one measurement. If we have two measurements, which give us different bounds on c_1, it is also possible to get bounds on c_2 without any assumptions on the microstructure. Geometrically, we fail to get bounds c_2 from one measurement, because the effective permittivity is (by construction) on the boundary of the $\epsilon_2^L/\epsilon_2^U$-bounds, when $c_1 = c_1^L$ or $c_1 = c_1^U$.

Assume that the measurement of $\epsilon^{\text{eff}}(\omega_0)$ give us tighter bounds $c_1^L(\omega_0) \leq c_1 \leq c_1^U(\omega_0)$ than the measurement of $\epsilon^{\text{eff}}(\omega_1)$. If we use the tighter bounds $c_1^L(\omega_0) \leq c_1 \leq c_1^U(\omega_0)$ together with the measurement $\epsilon^{\text{eff}}(\omega_1)$, we avoid the boundary and we can continue to bound c_2. This simple observation is the key to the construction of the bounds on any structural parameter.

To bound the c_1-dependent parameter c_2 with a fixed value on c_1 the equations

$$\epsilon^{\text{eff}}(\omega_1) = \epsilon_3^U(c_3, c_2; c_1(\omega_0)), \quad \epsilon^{\text{eff}}(\omega_1) = \epsilon_3^L(c_3, c_2; c_1(\omega_0)) \tag{3.33}$$

are solved in the range $c_1^{\mathrm{L}}(\omega_0) \leq c_1 \leq c_1^{\mathrm{U}}(\omega_0)$. By construction, the two lens-shaped regions $\epsilon_2^{\mathrm{L}}(c_2; c_1^{\mathrm{L}}, \omega_0)$, $\epsilon_2^{\mathrm{U}}(c_2; c_1^{\mathrm{L}}, \omega_0)$ and $\epsilon_2^{\mathrm{L}}(c_2; c_1^{\mathrm{U}}, \omega_0)$, $\epsilon_2^{\mathrm{U}}(c_2; c_1^{\mathrm{U}}, \omega_0)$ intersect, see Figure 6. From the bound ϵ_3^{U}, we get an upper bound $c_2^{\mathrm{U}}(c_1)$ on c_2 and the lower bound ϵ_3^{L} provide a lower bound $c_2^{\mathrm{U}}(c_1)$ on c_2.

We can now construct three-point bounds on ϵ^{eff} by forming

$$\epsilon_3^{\mathrm{L}}(c_3, c_2^{\mathrm{U}}(c_1), c_1), \quad \epsilon_3^{\mathrm{U}}(c_3, c_2^{\mathrm{L}}(c_1), c_1) \tag{3.34}$$

with $c_1 \in [c_1^{\mathrm{L}}(\omega_0), c_1^{\mathrm{U}}(\omega_0)]$ and $c_3 \in [c_3^{\min}, c_3^{\max}]$. The c_1-dependent maximum $c_3^{\max}$ and the minimum $c_3^{\max}$ are taken from the expression (3.3).

The upper bound $c_2^{\mathrm{U}}(c_1)$ and the lower bound $c_2^{\mathrm{L}}(c_1)$ are both second-degree polynomials in c_1, which are easily maximized and minimized. Global, c_1-independent, bounds on c_2 are defined as

$$c_2^{\mathrm{L}}(\omega_1) = \min_{c_1 \in [c_1^{\mathrm{L}}, c_1^{\mathrm{U}}]} \{c_2^{\mathrm{L}}(c_1)\}, \quad c_2^{\mathrm{U}}(\omega_1) = \max_{c_1 \in [c_1^{\mathrm{L}}, c_1^{\mathrm{U}}]} \{c_2^{\mathrm{U}}(c_1)\}. \tag{3.35}$$

If some of the structural parameters are known, for example, if the volume fraction is known and the material is isotropic, the two measurements give bounds on the higher order moments c_3 and c_4.

From the derivation of the maximum $c_3^{\max}$ and the minimum $c_3^{\min}$ in [19] we have the equalities $\epsilon_3^{\mathrm{L}} = \epsilon_2^{\mathrm{L}}$ when $c_3 = c_3^{\max}$ and $\epsilon_3^{\mathrm{L}} = \epsilon_2^{\mathrm{U}}$ when $c_3 = c_3^{\min}$. In the same way the upper bound ϵ_3^{U} can be used to limit the c_3-parameter. We obtain the equalities $\epsilon_3^{\mathrm{U}} = \epsilon_2^{\mathrm{L}}$ when $c_3 = c_3^{\max}$, and $\epsilon_3^{\mathrm{U}} = \epsilon_2^{\mathrm{U}}$ when $c_3 = c_3^{\min}$. Using these properties, the bounding region in (3.34), that depends on two variables c_1 and c_3 can be expressed as a set of bounds, depending on one single variable. The new bounds are

$$\epsilon_3^{\mathrm{U}}(c_3; c_2^{\mathrm{L}}(c_1^{\mathrm{U}}), c_1^{\mathrm{U}}), \quad \epsilon_3^{\mathrm{U}}(c_3; c_2^{\mathrm{L}}(c_1^{\mathrm{L}}), c_1^{\mathrm{L}}), \quad \epsilon_2^{\mathrm{U}}(c_1, c_2^{\mathrm{L}}(c_1)), \quad \epsilon_2^{\mathrm{L}}(c_1, c_2^{\mathrm{L}}(c_1)) \tag{3.36}$$

and

$$\epsilon_3^{\mathrm{L}}(c_3; c_2^{\mathrm{U}}(c_1^{\mathrm{U}}), c_1^{\mathrm{U}}), \quad \epsilon_3^{\mathrm{L}}(c_3; c_2^{\mathrm{U}}(c_1^{\mathrm{L}}), c_1^{\mathrm{L}}), \quad \epsilon_2^{\mathrm{U}}(c_1, c_2^{\mathrm{U}}(c_1)), \quad \epsilon_2^{\mathrm{L}}(c_1, c_2^{\mathrm{U}}(c_1)), \tag{3.37}$$

where the two-point bounds depend on $c_1 \in [c_1^{\mathrm{L}}(\omega_0), c_1^{\mathrm{U}}(\omega_0)]$ and the three-point bounds depend on $c_3 \in [c_3^{\min}, c_3^{\max}]$.

3.4 The checkerboard

We give an example of the method when no structural information is known using the checkerboard structure. Assume, as before, that $\epsilon_2(\omega_0) = 4.1 + 4.5\mathrm{i}$ and $\epsilon_2(\omega_1) = 4.6 + 0.06\mathrm{i}$ are known and that $\epsilon_1 = 3$ independent of the frequency ω. Moreover, we assume that $\epsilon^{\mathrm{eff}}(\omega_0)$ and $\epsilon^{\mathrm{eff}}(\omega_1)$ is measured and seek bounds on $\epsilon^{\mathrm{eff}}(\omega_2)$ when $\epsilon_2(\omega_2) = 3.7 + 0.04\mathrm{i}$ is known.

The second measurement on frequency ω_1 gives the tightest bounds on $c_1 = 0.5$,

$$c_1^{\mathrm{L}}(\omega_1) = 0.494, \quad c_1^{\mathrm{U}}(\omega_1) = 0.506. \tag{3.38}$$
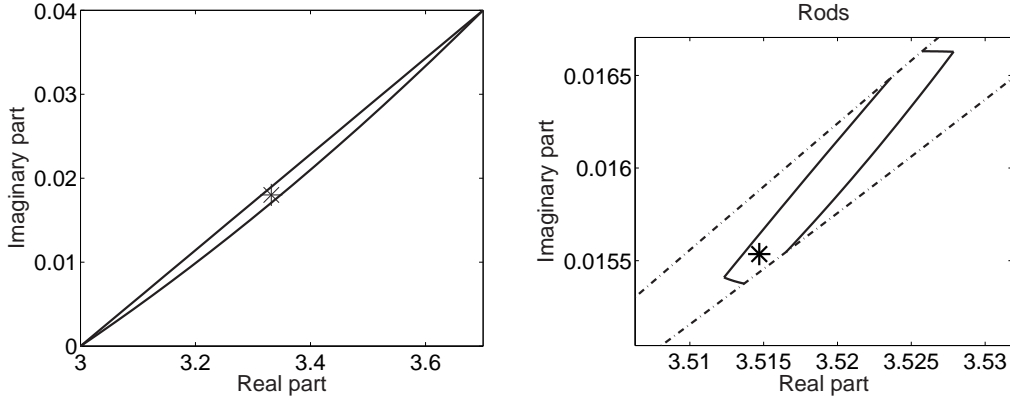
Figure 7: The star to the left is the location of the effective permittivity in the checkerboard case, and the star to the right corresponds to ϵ^{eff} for the rods. In both figures, the dash-dotted lines $\epsilon_2^{\text{L}}(c_2; c_1^{\text{L}})$ and $\epsilon_2^{\text{U}}(c_2; c_1^{\text{U}})$ bounds $\epsilon^{\text{eff}}(\omega_1)$ and the solid lines gives the tighter bounds (3.36) and (3.37).

We use the measurement of the effective permittivity on the frequency ω_0 to bound c_2. The solution to the equations $\epsilon^{\text{eff}}(\omega_0) = \epsilon_3^{\text{L}}$ and $\epsilon^{\text{eff}}(\omega_0) = \epsilon_3^{\text{U}}$, when $c_1 \in [c_1^{\text{L}}(\omega_1), c_1^{\text{U}}(\omega_1)]$ is

$$c_2^{\text{L}}(c_1) = 1.09296 - 6.0343c_1 + 7.15922c_1^2 \tag{3.39}$$

and

$$c_2^{\text{U}}(c_1) = -2.21787 + 7.28412c_1 - 6.15921c_1^2. \tag{3.40}$$

These functions have no stationary point when $c_1 \in [0.494, 0.506]$. The endpoints give the global bounds on $c_2 = -0.125$,

$$c_2^{\text{L}}(\omega_0) = -0.141, \quad c_2^{\text{U}}(\omega_0) = -0.108 \tag{3.41}$$

The bounds (3.36) and (3.37) that bounds $\epsilon^{\text{eff}}(\omega_1)$ are depicted in Figure 7.

3.5   An anisotropic example

Using the same material parameters as above, we also give an example in the anisotropic and periodic case, see Figure 8.

We use FEMLAB (www.comsol.com) to numerically calculate the solution to the local problem (2.2), (2.3). At the frequencies ω_0 and ω_1, the results are

$$\epsilon^{\text{eff}}(\omega_0) = 3.9426 + 0.9852i, \quad \epsilon^{\text{eff}}(\omega_1) = 3.5147 + 0.001554i. \tag{3.42}$$

The second measurement at the frequency ω_1 gives the tightest bounds on c_1,

$$c_1^{\text{L}}(\omega_1) = 0.5941, \quad c_1^{\text{U}}(\omega_1) = 0.6007 \tag{3.43}$$
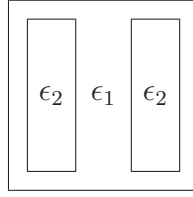
Figure 8: The geometry used to generate the result shown in Figure 7 and in Figure 9. Two rods with length 0.8 and width 0.25 are located, a distant 0.3 apart, in a unit square. The volume fraction is then $c_1 = 0.6$. The applied field is oriented perpendiculary to the rods.

We use the measurement of the effective permittivity on frequency ω_0 to bound c_2. The solution to the equations $\epsilon^{\text{eff}}(\omega_0) = \epsilon_3^{\text{L}}$ and $\epsilon^{\text{eff}}(\omega_0) = \epsilon_3^{\text{U}}$, when $c_1 \in [c_1^{\text{L}}(\omega_1), c_1^{\text{U}}(\omega_1)]$ are

$$c_2^{\text{L}}(c_1) = 7.07395 - 26.20256c_1 + 23.50343c_1^2 \tag{3.44}$$

and

$$c_2^{\text{U}}(c_1) = -2.46585 + 6.37039c_1 - 4.27488c_1^2. \tag{3.45}$$

These functions have no stationary point when $c_1 \in [0.5941, 0.6007]$. The endpoints give the global bounds

$$c_2^{\text{L}}(\omega_0) = -0.1974, \quad c_2^{\text{U}}(\omega_0) = -0.1817 \tag{3.46}$$

The bounds on $\epsilon^{\text{eff}}(\omega_2)$ when $\epsilon_2(\omega_2) = 3.7+0.04$i are known are depicted in Figure 7. The effective permittivity is numerically calculated to $\epsilon^{\text{eff}}(\omega_2) = 3.253 + 0.01306$i.

In practice, the effective permittivity (3.42) is the results of measurements and cannot in general be given with this accuracy. A computer program that takes in to account that measurements has errors have been written. If we assume that the error in the measurements of $\epsilon^{\text{eff}}(\omega)$ is 1%, the bounds on the volume fraction are numerically computed to

$$0.57 \leq c_1 \leq 0.62 \tag{3.47}$$

In a separate paper [18], the method derived here will be used to analyze data from real measurements.
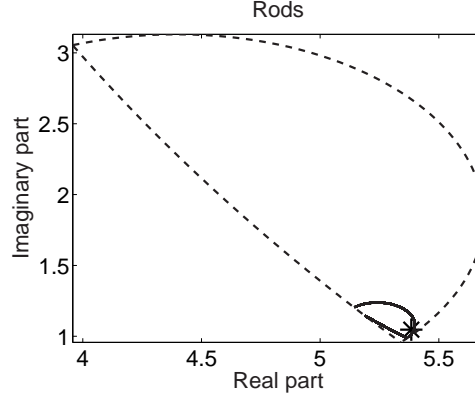
3.5.1 Bounds when the volume fraction is known

Assume that we have one measurement at ω_0 and one measurement at ω_2 (that here is numerically calculated in FEMLAB (`www.comsol.com`)). The effective permittivity at ω_2 is

$$\epsilon^{\text{eff}}(\omega_2) = 3.253 + 0.01306\text{i}. \tag{3.48}$$

The measurement at frequency ω_2 gives the tightest bounds on c_1,

$$c_1^{\text{L}}(\omega_2) = 0.5984, \quad c_1^{\text{U}}(\omega_2) = 0.6002. \tag{3.49}$$

Figure 9: The star is the effective permittivity $\epsilon^{\text{eff}}(\omega_3)$ bounded by the dashed lines $\epsilon_3^{\text{L}}(c_3; c_2^{\text{U}})$ and $\epsilon_3^{\text{U}}(c_3; c_2^{\text{L}})$. The solid lines are the tighter bounds $\epsilon_4^{\text{L}}(c_4, c_3^{\text{L}}(c_2))$ and $\epsilon_4^{\text{U}}(c_4, c_3^{\text{L}}(c_2))$.

The bounds on c_1 are in this case very tight. The arithmetic mean of $c_1^{\text{L}}(\omega_2)$ and $c_1^{\text{U}}(\omega_2)$ is then approximately $c_1^{\text{app}}(\omega_2) = 0.6$, which is the exact value on the volume fraction.

If $c_1 = 0.6$, is used the same schedule as above can be used to bound the parameters c_2 and c_3. The solution to the equations $\epsilon^{\text{eff}}(\omega_2) = \epsilon_3^{\text{L}}$ and $\epsilon^{\text{eff}}(\omega_2) = \epsilon_3^{\text{U}}$, with $c_1 = 0.6$ gives the tightest bounds on c_2,

$$c_2^{\text{L}}(\omega_2) = -0.18413, \quad c_1^{\text{U}}(\omega_2) = -0.18403. \tag{3.50}$$

The solution to the equations $\epsilon^{\text{eff}}(\omega_0) = \epsilon_4^{\text{L}}$ and $\epsilon^{\text{eff}}(\omega_0) = \epsilon_4^{\text{U}}$, with $c_2 \in [c_2^{\text{L}}(\omega_1), c_2^{\text{U}}(\omega_1)]$ is

$$c_3^{\text{L}}(c_2) = 1.37544 + 12.75996c_2 + 31.54795c_2^2 \tag{3.51}$$

and

$$c_3^{\text{U}}(c_2) = -7.60752 - 84.64558c_2 - 232.47525c_2^2 \tag{3.52}$$

These functions have no stationary point when $c_2 \in [c_2^{\text{L}}(\omega_1), c_2^{\text{U}}(\omega_1)]$. The endpoints give the global bounds

$$c_3^{\text{L}}(\omega_0) = 0.0955, \quad c_2^{\text{U}}(\omega_0) = 0.0966 \tag{3.53}$$

The bounds on $\epsilon^{\text{eff}}(\omega_2)$ were tight when the volume fraction was unknown, and they are now even tighter. We use a composite with larger contrast to illustrate the bounds. Assume that $\epsilon_1(\omega_3) = 3 + 0.1i$ and $\epsilon_2(\omega_3) = 2 + 20i$ are known. The bounds $\epsilon_4^{\text{L}}(c_4, c_3^{\text{L}}(c_2))$ and $\epsilon_4^{\text{U}}(c_4, c_3^{\text{L}}(c_2))$ on the effective permittivity $\epsilon^{\text{eff}}(\omega_3)$ are depicted in Figure 9. The effective permittivity is numerically calculated to $\epsilon^{\text{eff}}(\omega_3) = 5.409 + 1.038i$.

The geometry and the values on the phases were previously used in [19], where the value on the volume fraction c_1 and the anisotropy c_2 were assumed to be known. Here we obtain almost as tight bounds as in [19] by using the values of two measurements of a bulk property.

The bounds on c_2 from the measurement on ω_2 are close. If we use the arithmetic mean of $c_2^L(\omega_2)$ and $c_2^U(\omega_2)$ as an approximation, the same schedule can be used to bound the parameters c_3 and c_4.

4 Discussion and conclusions

We have developed a method to calculate inverse bounds on the structural parameters from measurements of lossy two-component composites. For example, measurements can be used to determine the frequency dependent effective permittivity.

If no structural information is known, data from two measurements determine bounds on the volume fraction and on the isotropy parameter. The bounds on the structural parameters are used to bound the permittivity at some frequency of interest or a related effective property, such as the electrical and thermal conductivity, magnetism, diffusion and flow in porous media.

In the case when some of the structural parameters are known, for example if the composite is known to be isotropic and the volume fraction is known, the same schedule can be used to bound higher order moments. The method can be extended to bound higher order moments, provided that we have information from more measurements of the bulk parameters.

Numerical experiments, with reasonable values for the permittivity, were used to illustrate the method.

5 Acknowledgements

References

[1] G. A. Baker. *Essentials of Padé Approximants*. Academic Press, New York, 1975.

[2] A. Bensoussan, J. L. Lions, and G. Papanicolaou. *Asymptotic Analysis for Periodic Structures*, volume 5 of *Studies in Mathematics and its Applications*. North-Holland, Amsterdam, 1978.

[3] M. J. Beran. Use of the variational approach to determine bounds for the effective permittivity in random media. *Nuovo Cimento*, **38**, 771–782, 1965.

[4] M. J. Beran. *Statistical Continuum Theories*. Interscience Publishers, New York, 1968.

[5] D. J. Bergman. Variational bounds on some bulk properties of a two-phase composite material. *Phys. Rev. B*, **14**(4), 1531–1542, 1976.

[6] D. J. Bergman. The dielectric constant of a composite material - a problem in classical physics. *Physical Reports*, **43**(9), 377–407, 1978.

[7] D. J. Bergman. Exactly solvable microscopic geometries and rigorous bounds for the complex dielectric constant of a two-component composite material. *Phys. Rev. Lett.*, **44**(19), 1285–1287, 1980.

[8] D. J. Bergman. Bounds for the complex dielectric constant of a two-component composite material. *Phys. Rev. B*, **23**(6), 3058–3065, 1981.

[9] D. J. Bergman. Hierarchies of Stieltjes functions and their application to the calculation of bounds for the dielectric constant of a two-component composite medium. *SIAM J. Appl. Math.*, **53**(4), 915–930, 1993.

[10] O. P. Bruno. The effective conductivity of strongly hetrogeneous composites. *Proceedings of the Royal Society of London. Series A, Mathematical and Physical Science*, **433**(1888), 353–381, 1991.

[11] E. Cherkaeva. Inverse homogenization for evaluation of effective properties of a mixture. *Inverse Problems*, **17**, 1203–1218, 2001.

[12] E. Cherkaeva and K. M. Golden. Inverse bounds for microstructural parameters of composite media derived from complex permittivity measurements. *Waves in Random Media*, **8**, 437–450, 1998.

[13] E. Cherkaeva and A. C. Tripp. Inverse conductivity for inaccurate measurements. *Inverse Problems*, **12**, 869–883, 1996.

[14] A. R. Day and M. F. Thorpe. The spectral function of random resistor networks. *J. Phys.–Condensed Matter*, **8**, 4389–4409, 1996.

[15] A. R. Day and M. F. Thorpe. The spectral function of composites: the inverse problem. *J. Phys.–Condensed Matter*, **11**, 2551–2568, 1999.

[16] A. R. Day, M. F. Thorpe, A. R. Grant, and A. J. Sievers. The spectral function of a composite from reflectance data. *Physica B*, **279**, 17–20, 2000.

[17] B. R. Djordjević, J. H. Hetherington, and M. F. Thorpe. Spectral function for a conducting sheet containing circular inclusions. *Phys. Rev. B*, **53**(22), 14862–14871, 1996.

[18] C. Engström. Structural information of composites from complex-valued, measured bulk properties. In preparation.

[19] C. Engström. Bounds on the effective tensor and the structural parameters for anisotropic two-phase composite material. *J. Phys. D: Applied Phys.*, **38**, 3695–3702, 2005.

[20] K. Golden and G. Papanicolaou. Bounds for effective parameters of heterogeneous media by analytic continuation. *Communications in Mathematical Physics*, **90**, 473–491, 1983.

[21] Z. Hashin and S. Shtrikman. A variational approach to the theory of the effective magnetic permeability of multiphase materials. *J. Appl Phys.*, **33**(10), 3125–3131, 1962.

[22] K. Hinsen and B. U. Felderhof. Dielectric constant of a suspension of uniform spheres. *Phys. Rev. B*, **46**(20), 12955–12963, 1992.

[23] V. V. Jikov, S. M. Kozlov, and O. A. Oleinik. *Homogenization of Differential Operators and Integral Functionals*. Springer-Verlag, Berlin, 1994.

[24] J. B. Keller. A theorem on the conductivity of a composite medium. *J. Math. Phys.*, **5**(4), 548–549, 1964.

[25] R. Lipton. Optimal inequalities for gradients of solutions of elliptic equations occurring in two-phase heat conduction. *SIAM J. Math. Anal.*, **32**(5), 1081–1093, 2001.

[26] K. A. Lurie and A. V. Cherkaev. Exact estimates of conductivity of composites. *Proc. Royal Soc. Edinburgh*, **A99**, 71–84, 1984.

[27] H. Ma, B. Zhang, W. Y. Tam, and P. Sheng. Dielectric-constant evaluation from microstructures. *Phys. Rev. B*, **61**(2), 962–966, 2000.

[28] J. C. Maxwell. *A Treatise on Electricity and Magnetism*, volume 1. Dover Publications, New York, 1954.

[29] R. C. McPhedran, D. R. McKenzie, and G. W. Milton. Extraction of structural information from measured transport properties of composites. *Applied Physics A*, **29**(1), 19–27, 1982.

[30] G. W. Milton. Bounds on the complex dielectric constant of a composite material. *Appl. Phys. Lett.*, **37**(3), 300–302, 1980.

[31] G. W. Milton. Bounds on the transport and optical properties of two-component composite material. *J. Appl Phys.*, **52**(8), 5294–5304, 1981.

[32] G. W. Milton. *The Theory of Composites*. Cambridge University Press, Cambridge, U.K., 2002.

[33] S. Prager. Improved variational bounds on some bulk properties of a two-phase random medium. *J. Chem. Phys.*, **50**(10), 4305–4312, 1969.

[34] K. Schulgasser. On a phase interchange relationship for composite materials. *J. Math. Phys.*, **17**, 378–381, 1976.

[35] A. K. Sen and S. Torquato. Effective conductivity of anisotropic two-phase composite media. *Phys. Rev. B*, **39**(7), 4504–4515, 1989.

[36] N. R. Silnutzer. *Effective constants of statistically homogeneous materials*. PhD thesis, University of Pennsylvania, Philadephia, 1972.

[37] L. Tartar. Estimations fines de coefficients homogénéisés. In P. Krée, editor, *Ennio De Giorgi Colloquium, Research Notes in Mathematics 125*, pages 168–187, 1985.

[38] S. Torquato. Effective electrical conductivity of two-phase disordered composite media. *J. Appl Phys.*, **58**(10), 3790–3797, 1985.

[39] O. Wiener. Die Theorie des Mischkörpers für das Feld des stationären Strömung. *Abh. Math. -Physichen Klasse Königl. Säcsh. Gesel. Wissen*, **32**, 509–604, 1912.